Crystal growth in colloidal tin oxide nanocrystals induced by coalescence at room temperature

E. R. Leite,[a] T. R. Giraldi, F. M. Pontes, and E. Longo
Department of Chemistry, Federal University of São Carlos (UFSCar), CP-676, São Carlos, SP, 13565-905, Brazil

A. Beltrán and J. Andrés
Departament de Ciències Experimentals, Universitat Jaume I, 12080 Castelló, Spain

The crystal growth process in colloidal nanocrystal systems is usually associated with the Ostwald-ripening mechanism. Here, we report on experimental evidence indicating that another crystal growth process took place in a colloidal nanocrystal system at room temperature. This crystal growth process is based on grain rotation among neighboring grains, resulting in a coherent grain–grain interface, which, by eliminating common boundaries, causes neighboring grains to coalesce, thereby forming a single larger nanocrystal. This phenomenon was observed in SnO_2 nanocrystals (particle size ranging from 10 to 30 Å). © *2003 American Institute of Physics.*
[DOI: 10.1063/1.1605241]

Crystal growth has been studied exhaustively and this topic has recently gained even greater importance due to the interest in controlling particle size in nanostructured materials.[1–5] Particle nucleation and growth are fundamental phenomena for the synthesis of metal, semiconductors, and metal oxide nanocrystals based on colloidal processes.[6] The solubility (S) of the particle formed during nucleation is related to the particle's size (d) by the Ostwald–Freundlich equation:

$$S = S_o \exp(4\gamma_{SL}V_m/RTd), \tag{1}$$

where S_o is the solubility of the flat surface, γ_{SL} is the solid–liquid interfacial energy, V_m is the molar volume of the solid phase, R is the gas constant, and T is the temperature. This dependence controls the nucleation and the growth process. Any particle system dispersed in a medium and having a certain degree of solubility in it is thermodynamically unstable due to its large interface area. Thus, one way of decreasing the high interfacial energy associated with this large interfacial area is through particle growth, and the mechanism most likely to achieve this reduction is Ostwald ripening.[7,8]

Moldovan and co-workers[3] recently studied the grain growth process of nanocrystalline materials and proposed a growth mechanism: grain-rotation-induced grain coalescence. According to this model, the rotation of grains among neighboring grains results in a coherent grain–grain interface (the grains assume the same crystallographic orientation), which leads to the coalescence of neighboring grains via the elimination of common grain boundaries, thus forming a single larger grain. In fact, this process had already been observed in colloidal systems under special conditions (usually, under hydrothermal condition) and was dubbed coarsening by oriented attachment.[9–11] The crystal growth process in this letter will be dubbed the grain-rotation-induced grain

coalescence (GRIGC) mechanism. We believe that this growth mechanism can take place in colloidal systems at room temperature. The jiggling of nanoparticles by the Brownian motion can allow adjacent particles to collide and rotate to find a low-energy configuration, resulting in a coherent grain–grain boundary. This phenomenon can occur even during particle deposition. Here, we give experimental evidence that the GRIGC mechanism is an important crystal growth process in colloidal tin oxide (SnO_2) nanocrystal at room temperature.

In order to obtain experimental results in support of this assumption, we have developed a synthesis method by which SnO_2 nanoparticles can be synthesized at room temperature, without requiring subsequent heat or hydrothermal treatment to promote crystallization. Our choice of SnO_2 as the test material was based on its very low solubility in the solvent used during synthesis, particularly at room temperature.[12] Low solubility and temperature are important factors to avoid the predominance of dissolution-based mechanisms such as the Ostwald-ripening mechanism. Besides, SnO_2 is a wide-band-gap semiconductor that presents interesting optical and electronic properties.[13]

SnO_2 nanocrystals with diameter size ranging from 10 to 30 Å were synthesized by a process involving the hydrolysis of $SnCl_2$ in an ethanol solution. No organic surfactant was used during the synthesis in order to avoid steric stabilization and surface contamination. The adsorption of organic molecules on the surface of SnO_2 nanocrystals can prevent particles from becoming attached to each other, inhibiting the GRIGC mechanism.[9] Coagulation of the particles in solution was prevented by using electrostatic stabilization through pH control. The as-prepared SnO_2 colloidal suspension was deposited in a copper-coated carbon grid for investigation by high-resolution transmission electron microscopy (HRTEM) (JEOL 3010 ARP microscope), with the microscope operated at an acceleration voltage of 300 kV. The colloidal suspension was deposited and dried in air to avoid the application of heat treatments.
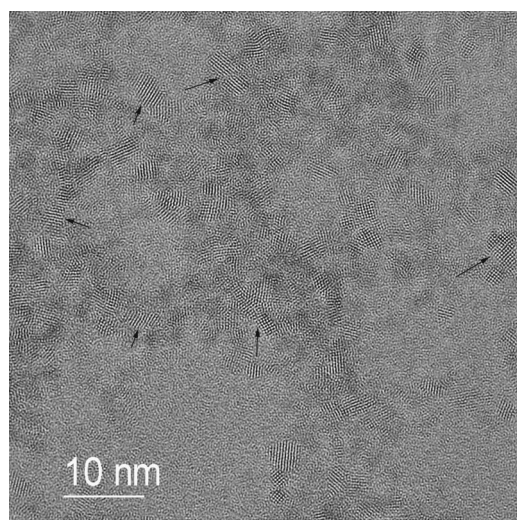
[a] Electronic mail: derl@power.ufscar.br

FIG. 1. Low-magnification HRTEM image of the SnO_2 particles deposited at room temperature. Arrows indicate the presence of clusters and grain chains.

Figure 1 shows a HRTEM image of the SnO_2 particles deposited at room temperature, revealing a material that is well crystallized even without heat treatment at high temperatures. The presence of crystalline SnO_2 with a rutile-type structure was confirmed by x-ray diffraction (XRD) analysis. This low-magnification HRTEM image shows randomly oriented particles, as well as several clusters and chains formed by grains with the same crystallographic orientation (indicated by arrows). As can be seen in Fig. 1, the presence of clusters and grain chains is quite frequent, suggesting the large-scale formation of such morphologies. A more-detailed analysis can be made based on the highly magnified HRTEM image in Fig. 2, which shows that the chain and the grain cluster [Figs. 2(a) and 2(c), respectively] are composed of several primary nanocrystals without grain boundaries. A fast Fourier transform (FFT) analysis of the two different regions of the chain [Fig. 2(a)] confirmed that the grains were similarly oriented. Figures 2(a) and 2(c) provide strong evidence that coalescence occurs when two or more grains assume the same orientation, resulting in a single crystalline cluster or chain. Observation of the coalescence process in a system not subjected to heat treatment suggests that this growth mechanism presents a very low activation energy or even a zero-kinetic barrier. Slight misorientations (indicated by arrows) are visible in the images of a cluster composed of several primary SnO_2 nanocrystals (at least four nanocrystals), shown in Fig. 2(c). These misorientations or defects originate from imperfect attachment among several nanocrystals, resulting in edge and screw dislocations. A substantial driving force for the crystal rotation to achieve perfectly coherent grain–grain boundaries is expected; however, some rotation may be metastable and preserved by the formation of a coincident site array. The imperfectly oriented attachment may produce different kinds of defects (e.g., dislocation from pure edge to pure screw), depending on the rotational relation of one nanocrystal to the others.[10] It is interesting to observe, in Fig. 2(b), that a tilt between the grains suffices to prevent coalescence. In fact, Fig. 2(b) shows the initial stage of the grain growth process. The arrow indicates the formation of necks between grains. An
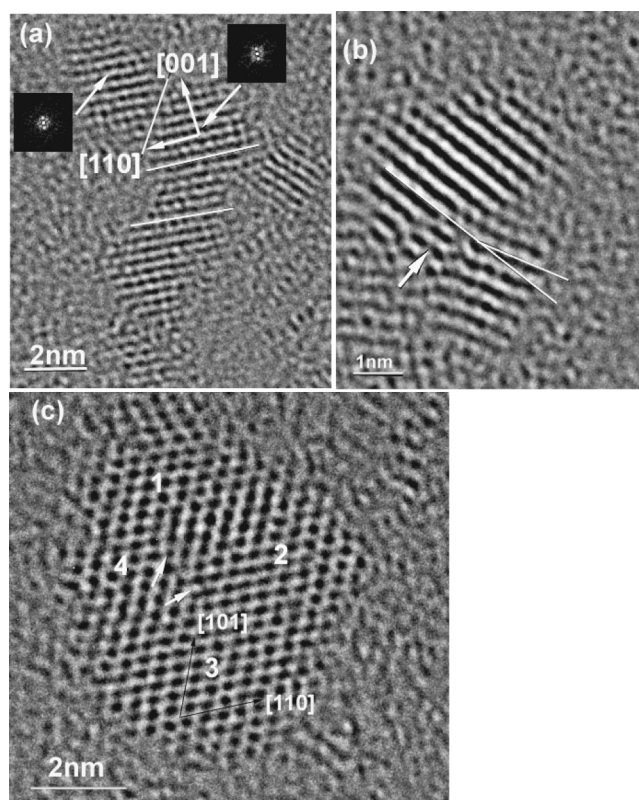

FIG. 2. High-magnification HRTEM image of SnO_2 nanocrystals. (a) Chain of SnO_2 composed of several nanocrystals. Insets show FFT analyses of the indicated area; (b) initial stage of the grain growth process; and (c) cluster composed of several SnO_2 nanocrystals.

analysis of Fig. 2(b) suggests that the first step in the grain growth process is the formation of necks. After this step, a rotation may occur to decrease the angle of misorientation, changing the grains' orientation. When the grains assume the same orientation, i.e., a coherent grain–grain boundary, the grain boundary must migrate toward the smaller particle,[14] resulting in a single larger crystalline nanocrystal.

The basic difference between the GRIGC mechanism and the Ostwald-ripening mechanism is illustrated schematically in Fig. 3. In the Ostwald-ripening mechanism [Fig. 3(a)], the atoms from one particle undergo dissolution and are then transferred to another particle. There is a net atomic transport from the particles with sizes smaller than the average value to larger particles. Particles smaller than the average value will shrink or even disappear. The GRIGC mechanism [Fig. 3(b)] occurs when two or more particles collide, promoting attachment between particles. This process of attachment is followed by a process of rotation, which leads to a low-energy configuration, thereby forming a coherent grain–grain boundary and eliminating the common grain boundary, resulting in a single larger nanocrystal (coalescence process).

The GRIGC mechanism is directly related to the reduction of surface energy, aimed at minimizing the area of high-energy faces.[9,10] Thus, an analysis of the surface energy in several crystallographic orientations can be useful to predict preferential growth directions. However, the surface energy of solids is usually not data available as experimental values. To circumvent this problem, we calculated the specific surface energy and its relative stability, using the crystalline
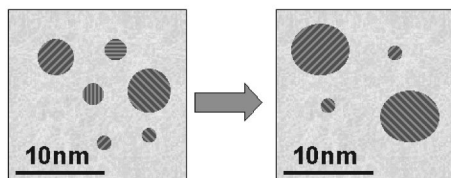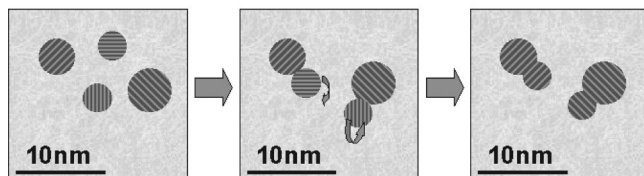
(a) Ostwald ripening

(b) Grain-rotation-induced grain coalescence (GRIGC)

FIG. 3. Schematic representation of the GRIGC and Ostwald-ripening mechanisms. (a) Representation of the Ostwald ripening mechanism; and (b) representation of the GRIGC mechanism. Arrows in the second block illustrate the rotation between grains.

orbital program Crystal-98.[15] This calculation was made within the framework of the density functional theory with the hybrid functional B3LYP.[16,17] The Sn and O centers are described in the schemes (DB)31G and (DB)-21G, respectively, where (DB) stands for the Durand–Barthelat nonrelativistic large effective core potential.[18] The specific surface energies calculated in several directions are listed in Table I and the results obtained from this study are compared with other results reported in the literature.[19,20] As expected, the (110) surface had the lowest surface energy and the (001) surface the highest among the surfaces considered. Based on this theoretical study, one can predict preferential growth along the [001]. An anisotropic growth may occur even in the [101] direction. For example, the surface energy of the (001) surface is 1.53 times greater than the (110) surface, while the (101) surface presents a surface energy only 1.19

TABLE I. Specific surfaces energies of SnO_2 rutile-like structures calculated in several surfaces.

Surface	Specific surface energy (J/m^2)		
	This work	Ref. 19	Ref. 20
(110)	1.2	1.04	1.40
(010),(100)	1.27	1.14	1.65
(101)	1.43	1.33	1.55
(201)	1.63	⋯	⋯
(001)	1.84	1.72	2.36

times that of the (110) surface. This analysis suggests that growth in the [001] direction will result in particles with a higher aspect ratio than growth in the [101] direction.

Our HRTEM results revealed the formation of chains and primary particle clusters resulting in a single large crystalline nanocrystal. The chain morphology showed preferential growth in the [001] direction, while the clusters grew preferentially in the [101] direction. These results, which indicate that the GRIGC mechanism occurs, typically, on high-surface-energy planes, are congruent with the theoretical calculations.

In summary, we have shown that the GRIGC mechanism occurs in SnO_2 nanocrystals at room temperature. Observing this mechanism at room temperature may elucidate, for instance, the presence of dislocations usually found in nanocrystals (see Fig. 2). The results presented herein may serve as important input for the development of nanostructured materials.

[1] C. T. Campbell, S. C. Parker, and D. E. Starr, Science **298**, 811 (2002).
[2] K. L. Merkle and L. J. Thompson, Phys. Rev. Lett. **88**, 225501 (2002).
[3] D. Moldovan, V. Yamakov, D. Wolf, and S. R. Phillport, Phys. Rev. Lett. **89**, 206101 (2002).
[4] E. R. Leite, I. T. Weber, E. Longo, and J. A. Varela, Adv. Mater. (Weinheim, Ger.) **12**, 965 (2000).
[5] E. R. Leite, A. P. Maciel, I. T. Weber, P. N. Lisboa-Filho, E. Longo, C. O. Paiva-Santos, A. V. C. Andrade, C. A. Paskocimas, Y. Maniette, and W. H. Schreiner, Adv. Mater. (Weinheim, Ger.) **14**, 905 (2002).
[6] E. R. Leite, in *Encyclopedia of Nanoscience and Nanotechnology*, edited by H. S. Nalwa (ASP, Stevenson Ranch, CA, 2003).
[7] R. D. Vengrenovitch, Acta Metall. **30**, 1079 (1982).
[8] J. M. Lifsitz, and V. V. Slezhov, Phys. Chem. Solids **19**, 35 (1961).
[9] R. L. Penn, and J. F. Banfield, Geochim. Cosmochim. Acta **63**, 1549 (1999).
[10] R. L. Penn, and J. F. Banfield, Science **281**, 969 (1998).
[11] J. F. Banfield, S. A. Welch, H. Zhang, T. T. Ebert, and R. L. Penn, Science **289**, 751 (2000).
[12] *CRC Handbook of Chemistry and Physics*, 72nd ed., edited by D. R. Lide (CRC, Boca Raton, FL, 1992).
[13] N. Chiodini, A. Paleari, D. DiMartino, and G. Spinolo, Appl. Phys. Lett. **81**, 1702 (2002).
[14] C. Greskovich, and K. W. Lay, J. Am. Ceram. Soc. **55**, 142 (1972).
[15] V. R. Saunders, R. Dovesi, C. Roetti, M. Causà, N. M. Harrison, R. Orlando, and C. M. Zicovich-Wilson, *CRYSTAL98 User's Manual* (University of Torino, Torino, 1998).
[16] A. D. Becke, J. Chem. Phys. **98**, 5648 (1993).
[17] C. Lee, W. Yang, and R. G. Parr, Phys. Rev. B **37**, 785 (1988).
[18] P. Duarnd and J. C. Barthelat, Theor. Chim. Acta **38**, 283 (1975)
[19] J. Oviedo, and M. J. Gillan, Surf. Sci. **463**, 93 (2000).
[20] B. Slater, C. R. A. Catlow, D. H. Gay, D. E. Williams, and V. Dusastre, J. Phys. Chem. B **103**, 10644 (1999).